energies

MDPI

Article

Optimal Under-Frequency Load Shedding Setting at Altai-Uliastai Regional Power System, Mongolia

Martha N. Acosta [1,2], Choidorj Adiyabazar [3], Francisco Gonzalez-Longatt [1,*], Manuel A. Andrade [2], José Rueda Torres [4], Ernesto Vazquez [2] and Jesús Manuel Riquelme Santos [5]

[1] Department of Electrical Engineering, Information Technology and Cybernetics, University of South-Eastern Norway, 3918 Porsgrunn, Norway; Martha.Acosta@usn.no

[2] School of Mechanical and Electrical Engineering, Universidad Autónoma de Nuevo León, San Nicolas de los Garza 66455, NL, Mexico; manuel.andradest@uanl.edu.mx (M.A.A.); evazquezmtz@gmail.com (E.V.)

[3] Power System Analysis and Research Department, National Dispatching Center Co. Ltd., Ulaanbaatar 17032, Mongolia; Choidorj.a@ndc.energy.mn

[4] Department of Electrical Sustainable Energy, Delft University of Technology (TU Delft), 2628 Delft, The Netherlands; J.L.RuedaTorres@tudelft.nl

[5] Department of Electrical Engineering, Universidad de Sevilla, 41004 Seville, Spain; jsantos@us.es

* Correspondence: fglongatt@fglongatt.org

Received: date; Accepted: date; Published: date

Abstract: The Altai-Uliastai regional power system (AURPS) is a regional power system radially interconnected to the power system of Mongolia. The 110 kV interconnection is exceptionally long and susceptible to frequent trips because of weather conditions. The load-rich and low-inertia AURPS must be islanded during interconnection outages, and the under-frequency load shedding (UFLS) scheme must act to ensure secure operation. Traditional UFLS over-sheds local demand, negatively affecting the local population, especially during the cold Mongolian winter season. This research paper proposes a novel methodology to optimally calculate the settings of the UFLS scheme, where each parameter of the scheme is individually adjusted to minimise the total amount of disconnected load. This paper presents a computationally efficient methodology that is illustrated in a specially created co-simulation environment (DIgSILENT® PowerFactory™ + Python). The results demonstrate an outstanding performance of the proposed approach when compared with the traditional one.

Keywords: frequency control; improved harmony search; metaheuristic algorithm; Mongolian power system; optimisation; under-frequency load shedding

1. Introduction

The power system continuously deals with power imbalances coming from fluctuations caused by imbalances between generation and demand. However, when the power system faces a severe power imbalance, such as the one caused by an abrupt increase of demand or a sudden disconnection of single/multiple generation units, several emergency control actions must be taken. One of those emergency control actions is under-frequency load shedding (UFLS) [1]. Its primary purpose is to stop the frequency from declining and to try and re-establish the balance between power demand and power generation by disconnecting an appropriate amount of load [2].

The classical automatic UFLS scheme uses under-frequency relays (UFRs), which are designed to operate any time the frequency drops below a predefined threshold using the instantaneous value of the local frequency [3]. The classical load shedding (LS) is performed at the same location where the frequency is sensed, and it can be done over one or multiple steps. The implementation of the

classical UFLS scheme implies identifying the most severe possible power imbalance and estimating the total amount of load disconnection, ensuring the frequency recovers above a minimum permissible value [4]. Once the total amount of LS is calculated, the parameters of the UFRs (number of load shedding stages, block size of load to be shed, frequency threshold and the time delay for each stage) must be set [5]. Typically, power system operators determine the fixed settings of UFRs using a trial and error procedure based on experience [3].

All parameters of UFRs require careful calculation, but the block size of LS and the number of LS steps require special attention. If these two parameters have inappropriate settings, it can cause undesirable results: (i) over-frequency conditions and/or loss of power service continuity produced by excessive LS at the initial stages of the frequency response and (ii) inability to arrest the frequency drop, leading to further loss of generation units or even system-wide blackout, produced by underestimated load shedding in the initial stages. Therefore, the total amount of LS is an extremely important factor for security and economic operation of a power system [6,7].

The main disadvantage of implementing the UFLS scheme using the traditional method is that errors can easily be made at the time when parameters of the UFRs are set. This is because the number of parameters to compute increases as the number of UFRs connected to the system increases, thereby becoming a complex problem and increasing the risk of inappropriate performance.

Although there are a vast number of methodologies to implement the traditional UFLS scheme that propose several sets of parameters depending on the country/company utility requirements [8–11], recent methods have focused on solving the problem of calculating the UFR parameters using computational algorithms. Authors of [12] used the genetic algorithm to minimise the LS and the dynamic frequency deviation of the power system. In [13], an adaptative UFLS scheme based on an artificial neuronal network (ANN) was proposed to estimate the power imbalance and then define the settings of UFRs. In [14], a methodology that combines UFLS with online fuzzy control strategy was presented to reduce the LS value. The authors of [15] introduced a method to compute the optimal values of load shedding, frequency threshold and time delay considering the high penetration of renewable generation resources. In [16], a technique was presented to assess the optimal load capacity and load disconnection sequence during a power system emergency. The particle swarm optimisation (PSO) algorithm has been implemented to estimate the amount of power imbalance and then calculate the size of LS [17], to solve a multi-objective function and determine the optimal amount of LS [18], and to compute the optimal amount of LS in an islanded operation scenario [19]. The trajectory sensitivity technique has been used to minimise the total LS cost of the power system [20]. Meanwhile, wide-area measurements (WAMs) have been used to create an intelligent UFLS scheme. For instance, the authors of [21] introduced a method based on artificial intelligence (AI) techniques and WAMs to calculate the optimal UFLS settings, [22] proposed an intelligent under-frequency and under-voltage scheme using WAMs to recover the frequency and voltage and the authors of [23] presented an adaptative UFLS model based on WAM information to set up an emergency LS strategy. Furthermore, several techniques are focused on addressing the effect of the measurement time delay on the performance of UFLS schemes [24–26]. A detailed literature review of the UFLS scheme is out of scope of this paper. For further information, the authors of [27] have presented a comprehensive analysis of UFLS schemes available in the literature.

The main drawback of most of the previous methodologies is that they assume the settings are the same for all UFRs as it can be a practical way to simplify the optimisation problem. However, that assumption can overestimate the total amount of load shedding and the frequency recovery because each load has a different active power value. Even if all the UFRs are set with the same block size of load shedding, the resulting load to be disconnected will be different. This fact can produce an over-frequency condition.

Moreover, another drawback of several methodologies, such as [14,18,19,21,22], is that they simplify the optimisation problem by considering only the block size of LS as a control variable and keep the number of load shedding stages, frequency threshold and time delay as fixed values. However, not considering all parameters of UFRs limits the solution of the optimisation problem and

can produce a wrong estimation of the optimal settings because the number of load shedding stages, frequency threshold and time delay have an impact on the frequency response.

The main objective of this research paper was to overcome the disadvantages of existing methodologies by introducing a novel method to optimally calculate the settings of the UFLS scheme. In this new approach, the principal parameters of the UFRs (number of load shedding stages, block size of load shedding, frequency threshold and the time delay for each stage) are considered in order to minimise the total amount of disconnected load. The significant contributions unfolding from this paper are listed below:

- The proposed methodology was formulated to consider and individually adjust each parameter of each UFR (number of load shedding stages, block size of load shedding, frequency threshold and the time delay for each stage) of the UFLS scheme. Thus, it allows all parameters that impact the frequency response to be taken into account, therefore obtaining the optimal settings and avoiding over/under load disconnection.
- A co-simulation framework (DIgSILENT® PowerFactory™ + Python) dedicated to performing optimisation of the UFLS scheme was developed by implementing the improved harmony search metaheuristic algorithm in Python and using time-domain simulations and discrete events from DIgSILENT® PowerFactory™.
- The optimal UFLS scheme was tested in the Altai-Uliastai regional power system of Mongolia. It was modelled in DIgSILENT® PowerFactory™ using the data of the real system. Simulation results showed the optimal UFLS scheme had superior performance compared to the traditional scheme currently installed in the Altai-Uliastai regional power system.
- The optimal settings of the UFLS scheme were assessed by carrying out a sensitivity analysis to ensure the optimisation reached the optimal solution.

The remainder of the paper is organised as follows. Section 2 presents a brief description of the Mongolian power system as well as the Altai-Uliastai regional power system. Section 3 introduces the implementation principles of the traditional UFLS scheme and describes the main characteristics of the Altai-Uliastai regional power system's UFLS scheme. Section 4 gives a detailed description of the formulation of optimal UFLS proposed in this research work. Section 5 depicts the methodology used to implement optimal UFLS, including a brief review of the optimisation method used. Section 6 describes the test system and the case studies used to assess the proposed methodology. Section 7 presents the results and the sensitivity analysis of the optimal setting. Finally, Section 8 presents the principal observations and conclusions.

2. Mongolian Power System

2.1. Overview of the MPS

The Mongolia power system (MPS) is an unbundled grid containing five regional power systems (RPS) as shown in Figure 1: (i) Central (CRPS), (ii) Western (WRPS), (iii) Altai-Uliastai (AURPS), (iv) Eastern (ERPS) and (v) Southern (SRPS). The MPS produces around 85% of its total electricity using coal-fired power plants, and the remaining 15% is supplied by renewable energy sources (RES), including hydro, wind and solar power plants. Furthermore, the MPS is composed of nine thermal power plants, three wind power plants, five solar power plants and three hydropower plants. The interconnection between the five RPS of the MPS is through 220 and 110 kV overhead transmission lines [28,29]. CRPS is the most extensive local energy system and is connected to AURPS, ERPS and SRPS through a 110 kV transmission line. In addition, CRPS has an interconnection with the Russian power system through a 220 kV double-circuit transmission line.

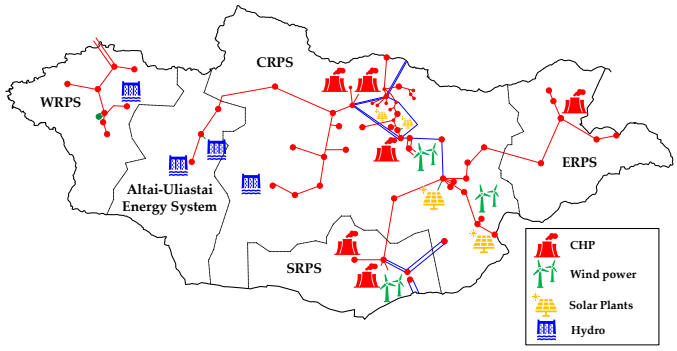

Figure 1. Representation of the Mongolia power system (MPS) indicating the main generation and transmission infrastructure.

The weather of Mongolia strongly influences the power consumption in the MPS, and the grid is operated considering two main seasons: winter and summer. Winter season is considered to start from the second half of September and lasts until the first half of May. In this season, temperatures reach values below −35 °C, and it is necessary to use central heating system. This causes high demand and requires a large number of generation units to be on service; therefore, the total rotational inertia of the MPS is high. On the other hand, the summer season starts in the second half of May and lasts until the first half of September. During this time, the central heating system is stopped, and the power demand reaches its minimum values. As the demand is reduced, several big power plants are scheduled to be out of service for maintenance purposes, and the total rotational inertia significantly decreases.

2.2. Altai-Uliastai Regional Power System

AURPS is as one of the five RPS of the MPS; it started to operate in 2009. It consists of six hydropower plants supplying electricity to 31 provinces and two towns. The largest hydropower plant of AURPS is Taishir with an installed capacity of 11 MW. Figure 2 depicts the main power generation and transmission infrastructure (actual model used in this paper).

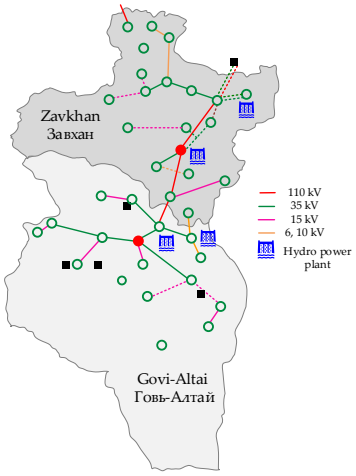

Figure 2. Representation of Altai-Uliastai regional power system (AURPS) indicating the main hydropower plants and transmission infrastructure.

The hydropower production at Altai-Uliastai depends on the water levels, and it operates on an average load of between 3.5 and 4.1 MW. The AURPS generates 49%–55% of the total consumption in the region, and the remaining percentage is imported from CRPS through the Murun-Telmen 110 kV transmission line. During the winter season, the small hydropower plants are out of services due to the freezing of rivers; therefore, the power supply in AURPS is critically dependent on power importation from CRPS. A summary of the power balance at AURPS during summer and winter

seasons are shown in Table 1 [29]. It is important to observe that the interconnection between AURPS and CRPS is essential as it provides 38.4% and 83.40% of the total demand for summer and winter seasons, respectively.

Table 1. Winter and summer operational scenarios of AURPS.

Season	Inertia/Demand Level	Production, P_G (MW)	Demand, P_D (MW)	Power Import from CRPS, P_{tie} (MW)
Summer	High/Low	4.6	6.25	2.4
Winter	Low/High	3.0	11.99	10.0

The winter season is a special concern because of low local generation and high demand, making the disconnection of the Murun-Telmen transmission line a critical loss of infeed.

3. Under-Frequency Load Shedding Scheme

3.1. Definition of UFLS Scheme

The implementation of the traditional UFLS scheme is based on setting the values of the parameters of all UFRs installed in the power system. The UFRs are mainly characterised by four parameters (see Figure 3) [4]: (i) the number of stages (N_s) or steps in which the UFR will disconnect the locally connected load, (ii) the block size of LS (ΔP) that will be disconnected at each stage (this value is based on the total load that is locally connected), (iii) the frequency threshold (f_T) at which the load must be shed in each stage and (iv) the time delay (t_d) between activating the consecutive stages.

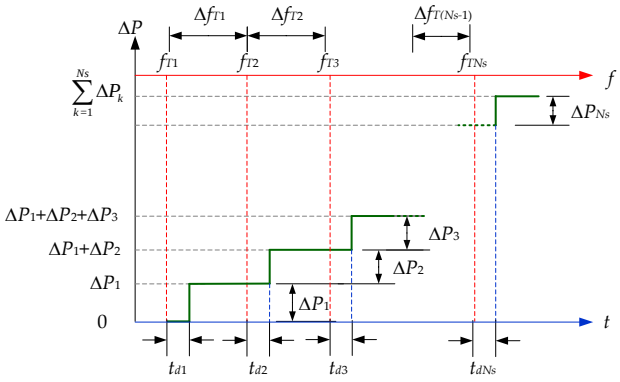

Figure 3. Power–frequency–time (*P*–*f*–*t*) schematic representation of the settings of an under-frequency relay (UFR).

Assuming that the power system has N_{UFR} UFRs installed, the settings of the i-th UFR (i = 1, 2, …, N_{UFR}) are mathematically described as follows:

$$\mathbf{\Delta P}_i = \left[\Delta P_{1,i} \quad \Delta P_{2,i} \quad \ldots \quad \Delta P_{k,i} \quad \ldots \quad \Delta P_{N_s,i} \right]_{1\times N_s} \tag{1}$$

$$\mathbf{F}_i = \left[f_{T1,i} \quad f_{T2,i} \quad \ldots \quad f_{Tk,i} \quad \ldots \quad f_{TN_s,i} \right]_{1\times N_s} \tag{2}$$

$$\mathbf{T}_i = \left[t_{d1,i} \quad t_{d2,i} \quad \ldots \quad t_{dk,i} \quad \ldots \quad t_{dN_s,i} \right]_{1\times N_s} \tag{3}$$

where $\Delta P_{k,i}$ defines the block size of LS, $f_{Tk,i}$ represent the frequency threshold and $t_{dk,i}$ is the time delay of the k-th stage in the i-th UFR. The process to calculate the four settings of each UFR becomes complex as the number of UFRs installed in the power system increases. This complexity is due to the fact that 3 × N_s parameters must be computed for each UFR, and the total number of parameters to be computed in the power system is (3N_s + 1) × N_{UFR}.

The correct performance of the UFLS scheme relies on the appropriate calculation of a set of settings, and this is dependent on considering (appropriately) the power system dynamic. Therefore, several factors must be considered in the procedure to implement the UFLS scheme. The UFLS must limit the maximum frequency deviation (Δf) as well as the depth of the frequency response (f_{nadir}) to protect the turbine generator units from prolonged under/low-frequency conditions. Consequently, it is essential to coordinate the UFLS scheme with under-frequency protection of the turbine generator units. Moreover, the UFLS must consider a reasonable margin between the nominal frequency (f_0) and the frequency threshold of the first stage (f_{T1}) to avoid activating the UFRs on non-emergency frequency conditions. After the UFRs action, the frequency will settle at a certain value depending on the initial overload and the load reduction per frequency reduction. Thus, UFLS must consider the actions of other controllers and/or the actions of system operators to avoid over-frequency scenarios after UFR activation. All these considerations raise the necessity of adopting techniques that facilitate the computation of UFR parameters and obtaining optimal settings to ensure the security of the power system by avoiding over/under shedding when the UFRs are activated.

3.2. UFLS Scheme in AURPS

The MPS uses a decentralised conventional UFLS scheme based on an automatic static UFR (ANSI number 81) taking measurements at each local placement. The traditional UFLS scheme at AURPS is adjusted to arrest the frequency before 47 Hz by disconnecting a maximum of 55% of the total demand, thus avoiding activation of under-frequency protection of the generation units, which are set at 46 Hz. Typically, the frequency threshold (f_T) is in the interval from 49.4 to 47.2 Hz, the time delay (t_d) is adjusted between 6 and 18 cycles and the number of steps is nine. Table 2 shows the settings used in the existing UFLS scheme in AURPS.

Table 2. Actual traditional UFLS settings of AURPS.

UFR Location	Element	ΔP (%)	f_T (Hz)	t_d (s)
Baynshand	Load	28	48.0	0.15
Baynhairhan	Load	55	47.8	0.15
Jargalant	Load	50	47.8	0.15
Uildwer	Load	87	47.8	0.15
Harzat	Load	55	47.8	0.15
Uliastai	Line	Open	48.8	0.10
Guulin [1]	Line	Open	48.0	0.15
Biger garaa [1]	Line	Open	48.0	0.10

[1] Out of service in the winter season.

4. Optimal UFLS Scheme

The UFLS scheme can be formulated as a mathematical optimisation problem seeking to obtain the optimal settings of the UFRs by considering an objective function. In this research paper, the objective of computing the UFLS settings at AURPS was to minimise the total load disconnection and at the same time ensure the security of the power system by stopping frequency decline after a significant system frequency disturbance. The formulation of the UFLS optimisation problem consisted of defining the mathematical expression for the objective function by considering a set of variables that impacts the frequency response and the operational requirements of the power system.

4.1. Frequency Quality Metrics

The metrics of the frequency during the primary frequency response (typically within the first 10–30 s after a frequency event occurs) are the time (t_{min}) at which the frequency reaches its maximum depth, called minimum instantaneous frequency (f_{min}) or frequency nadir, and the value at which the frequency settles, known as steady-state frequency (f_{ss}) [30,31]. After a system frequency disturbance,

in addition to the amount of rotational inertia available in the power system, the action of the UFRs directly influences the metrics of the frequency response, namely, the total amount of load shedding, the frequency threshold and the time delay impact on the values of f_{min} and t_{min}. Meanwhile, the total amount of load shedding mainly determines the level at which the frequency will settle (f_{ss}). Therefore, in a general approach, the UFLS parameters N_s, ΔP, f_T and t_d, the interval between two frequency thresholds (Δf_T) and even the best placement of the UFRs can be taken as frequency control variables at the time to formulate the UFLS as an optimisation problem.

The four main settings of each UFR—number of stages (N_s), block size of load shedding ($\Delta\mathbf{P}$), frequency threshold ($\mathbf{F}$) and time delay ($\mathbf{T}$)—are used as frequency control variables to solve the UFLS optimisation problem. Therefore, the frequency control variables vector ($\mathbf{x}_{FC}$) is mathematically written as follows:

$$\mathbf{x}_{\mathrm{FC}} = \begin{bmatrix} \mathbf{x}_1 & \mathbf{x}_2 & \dots & \mathbf{x}_i & \dots & \mathbf{x}_{N_{UFR}} \end{bmatrix}_{1\times(N_{UFR}\times 3N_s)} \tag{4}$$

$$\mathbf{x}_i = \begin{bmatrix} \Delta\mathbf{P}_i & \mathbf{F}_i & \mathbf{T}_i \end{bmatrix}_{1\times 3N_s} \quad \forall i = 1,2,\dots,N_{UFR} \tag{5}$$

and $\Delta\mathbf{P}_i$, $\mathbf{F}_i$ and $\mathbf{T}_i$ are defined in (1)–(3), containing a total number of frequency control variables of $N = 3N_{FR} \times N_s$.

Transmission system operators (TSOs) define several boundaries for UFR parameters according to the operational requirements of the power system. As a consequence, the frequency control variables are bounded as follows:

$$\begin{aligned} &\Delta\mathbf{P}_{\min} < \Delta\mathbf{P}_i < \Delta\mathbf{P}_{\max} \\ &\mathbf{F}_{\min} < \mathbf{F}_i < \mathbf{F}_{\max} \qquad \forall i = 1,2,\dots,N_{UFR} \\ &\mathbf{T}_{\min} < \mathbf{T}_i < \mathbf{T}_{\max} \end{aligned} \tag{6}$$

where $\Delta\mathbf{P}_{\min}$, $\mathbf{F}_{\min}$ and $\mathbf{T}_{\min}$ are the minimum limits of the block size of LS, frequency threshold and the time delay, respectively. Moreover, $\Delta\mathbf{P}_{\max}$, $\mathbf{F}_{\max}$ and $\mathbf{T}_{\max}$ represent the maximum limit of the block size of LS, frequency threshold and the time delay, respectively.

4.2. Objective Function

The main objective of optimising the settings of UFRs is to minimise the total amount of load shedding after an under-frequency disturbance occurs in order to recover the frequency into allowable values and avoid over/under LS conditions produced by wrong settings of the UFLS scheme. The objective function is defined as the sum of all active power disconnected by the UFRs, and it is written as follows:

$$\min_{\mathbf{x}}\left[f(\mathbf{x}_{\mathrm{FC}}) \right] = \min_{\mathbf{x}}\left[P_{LS}\left(\mathbf{x}_{\mathrm{FC}}\right) \right] = \sum_{i=1}^{N_{UFR}} \sum_{k=1}^{N_{sT}} \Delta P_{k,i} P_{L,i} \tag{7}$$

where $P_{L,i}$ is the total active power of the load controlled by the i-th UFR, $\Delta P_{k,i}$ is the block size of LS (% of $P_{L,i}$) at the k-th activated stage of the i-th UFR and N_{sT} is the number of triggered stages during the under-frequency event. Be aware that N_{sT} can be smaller or equal to N_s.

4.3. Operational Frequency Requirements

Although the main purpose of optimising the settings of the UFRs is to minimise the total amount of load shedding (P_{LS}), the frequency of the power system must fulfil specific operational requirements after the action of the UFLS scheme, i.e., frequency quality metrics being inside certain limits. Therefore, the operational frequency requirements are included in the optimisation problem as a set of inequality constraints based on two frequency quality metrics: minimum frequency (f_{min}) and the steady-state frequency (f_{ss}).

4.3.1. Minimum Frequency

After a disturbance, if the frequency falls too deep, the under-frequency protection (UFP) of the synchronous generator can be activated and premature generator tripping before system load shedding may occur, ultimately leading to unnecessary system collapse. Therefore, it is essential to coordinate the UFLS scheme with the UFP of generators. This can be done by ensuring that the minimum frequency (f_{min}) does not reach the operating zone of the UFP of generators. This condition can be written as follows:

$$\begin{aligned} &\mathbf{g}_{\alpha}\left(\mathbf{x}_{\mathrm{FC}}\right)=\left[\begin{array}{cccccc} g_{\alpha,1} & g_{\alpha,2} & \cdots & g_{\alpha,i} & \cdots & g_{\alpha,N_{UFR}} \end{array}\right]_{1\times N_{UFR}} \\ &g_{\alpha,i}=f_{limit}-f_{min,i} \quad \forall\, i=1,\ldots N_{UFR} \end{aligned} \tag{8}$$

where f_{limit} represents frequency limit before the operating zone of UFP of the generators.

4.3.2. Steady-State Constraint

Turbine generator units have load operating limitations during abnormal frequency conditions to avoid exposing the turbine blades from stress and increasing their lifetime. For instance, at 50 Hz nominal frequency, turbine generator units must be protected from prolonged operation below 49.2 Hz [32,33]. Consequently, the continuous operation of turbine generator units requires the steady-state frequency (f_{ss}) to be inside specific limits as follows:

$$f_{ss,\min} \le f_{ss} \le f_{ss,\max} \tag{9}$$

where $f_{ss,\min}$ and $f_{ss,\max}$ are the minimum and maximum limits of f_{ss}. This restriction is formulated as two inequality constraints as follows:

$$\begin{aligned} &\mathbf{g}_{\beta}\left(\mathbf{x}_{\mathrm{FC}}\right)=\left[\begin{array}{cccccc} g_{\beta,1} & g_{\beta,2} & \cdots & g_{\beta,i} & \cdots & g_{\beta,N_{UFR}} \end{array}\right]_{1\times N_{UFR}} \\ &g_{\beta,i}=f_{ss,i}-f_{ss,\max} \quad \forall\, i=1,\ldots N_{UFR} \end{aligned} \tag{10}$$

and

$$\begin{aligned} &\mathbf{g}_{\gamma}\left(\mathbf{x}_{\mathrm{FC}}\right)=\left[\begin{array}{cccccc} g_{\gamma,1} & g_{\gamma,2} & \cdots & g_{\gamma,i} & \cdots & g_{\gamma,N_{UFR}} \end{array}\right]_{1\times N_{UFR}} \\ &g_{\gamma,i}=f_{ss,\min}-f_{ss,i} \quad \forall\, i=1,\ldots N_{UFR} \end{aligned} \tag{11}$$

The vector $\mathbf{G}(x_{\mathrm{FC}})$ contains the inequality constraints defined in (8), (10) and (11), and it is defined as follows:

$$\mathbf{G}(\mathbf{x}_{\mathrm{FC}})=\left[\begin{array}{ccc} \mathbf{g}_{\alpha}(\mathbf{x}_{\mathrm{FC}}) & \mathbf{g}_{\beta}(\mathbf{x}_{\mathrm{FC}}) & \mathbf{g}_{\gamma}(\mathbf{x}_{\mathrm{FC}}) \end{array}\right]_{1\times(3N_{FR})} \le 0 \tag{12}$$

where the total number of inequality constraints of the UFLS optimisation problem is $N_{\mathrm{ineq}} = 3N_{FR}$.

5. Optimisation Framework

This section is dedicated to giving a brief description of the improved harmony search metaheuristic algorithm used to solve the UFLS problem. Furthermore, the optimisation framework developed to calculate the optimal UFLS scheme, which mainly consists of the interface of PowerFactory™+ Python, is presented.

5.1. Optimisation Algorithm: Improved Harmony Search (IHS)

IHS is a metaheuristic algorithm based on the harmony search algorithm proposed by Geem et al. [34]. The IHS algorithm is focused on the musical composition process. It mimics the procedure that musicians follow to improvise new pitches and create harmonies until they find the best harmony. The improvised pitches are represented by the set of variables of the optimisation problem, and the best harmony is the set of variables that produces the optimal solution by evaluating the

objective function [34]. First, the IHS algorithm is initialised by randomly creating a harmony (set of pitches), the harmony is used to evaluate the objective function and it is stored in a memory called harmony memory (HM). Then, a new harmony is improvised using the following criteria: selecting new pitches from the HM or creating them randomly. The new harmony is compared against the worst harmony stored in the HM; the HM is updated if the new harmony is better than the worst harmony in term of objective function evaluation. The IHS algorithm stops until it reaches a predefined number of improvisations (*NI*) [35]. This algorithm requires several parameters to be initialised: (i) the number of improvisations (*NI*), which determines the number of times the objective function will be evaluated; (ii) the harmony memory size (*HMS*), which defines the number of harmonies that will be stored in the HM; (iii) the harmony memory considering rate (*HCMR*), which is the probability of choosing the new pitches from HM; (iv) the pitch adjustment rate (*PAR*), which is the maximum (PAR_{max}) and minimum (PAR_{min}) probability of adjusting the new pith when it is selected from the HM and (v) the maximum (bw_{max}) and the minimum (bw_{min}) bandwidth distance [35].

5.2. Co-Simulation Framework: PowerFactory+ Python

The optimal UFLS scheme formulated in Section 4 was solved using the IHS algorithm, and the practical implementation required co-simulation between two subsystems: one dedicated to obtaining the system frequency response of the power system and another dedicated to iteratively solving the numerical optimisation problem (see Figure 4).

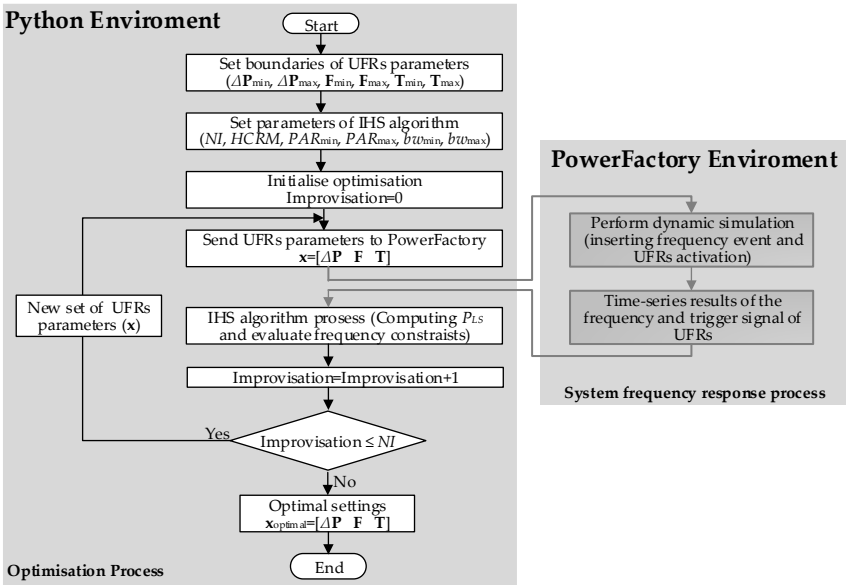

Figure 4. Co-simulation framework for optimal UFLS scheme.

The core of the co-simulation framework for optimal UFLS scheme is the optimisation process inside the python environment. It was implemented in the general-purpose programming language Python, and the IHS algorithm was taken from a scientific Python library (PyGMO), built to bring massive parallel optimisation interface [36]. The framework was complemented using DIgSILENT® PowerFactory™, which performed time-domain simulations and produced time-series of the electrical variables (frequency, active power) and discrete events (insert a disturbance, activation of UFRs).

The optimisation was performed using Python in an automatised close loop with PowerFactory™. For each improvisation, the UFR settings were taken from the optimisation output and placed on the UFRs in the power system model inside PowerFactory™. Then, a time-domain simulation, including the discrete events, was performed by PowerFactory. The dynamic response of the frequency and trigger signal of each stage of UFRs were interpreted at a high level by Python and

used to compute the objective function and evaluate the frequency operational requirements. The simulation stopped when the pre-set number of improvisations (*NI*) was reached. The pseudocode of the IHS algorithm is presented in Algorithm 1.

Algorithm 1. Improved Harmony Search Algorithm.

1: Initialise the IHS parameters: k, NI, HMS, $HMCR$, PAR_{min}, PAR_{max}, bw_{min} and bw_{max}.
2: HM = random(HMS, n) % Initialise the harmony memory
3: **while** ($k < NI$):
4: **for** j **in range**(0, n)
5: **if** rand(0,1) ≤ $HMCR$ %Harmony memory selection
6: j = randint(1, HMS)
7: x_{new} = HM(j,:)
8: $PAR_k = PAR_{min} + (PAR_{max} - PAR_{min}/NI) * k$
9: **if** rand() ≤ PAR_k % pitch adjustment
10: $bw_k = bw_{max} * \exp((\ln(bw_{min}/bw_{max})/NI) * k)$
11: $x_{new} = x_{new} + \text{rand}(-1,1) * bw_k$
12: **else** % Random selection
13: x_{new} = rand(x_L, x_U)
14: x(k,:) = x_{new}
15: **if** f(x) ≤ f(x$_{worst}$) %update the harmony memory
16: x$_{worst}$ = x
17: $k = k+1$ %Stopping criteria
18: **end**

6. Description of the Test System

The real model of the AURPS was implemented in DIgSILENT® PowerFactory™ version 2020, and it was used to obtain the optimal settings of UFRs of the UFLS scheme. The schematic single-line diagram of the AURPS is shown in Figure 5. It consists of 46 loads, 39 lines, 25 two-winding transformers, six three-winding transformers and 13 synchronous generators.

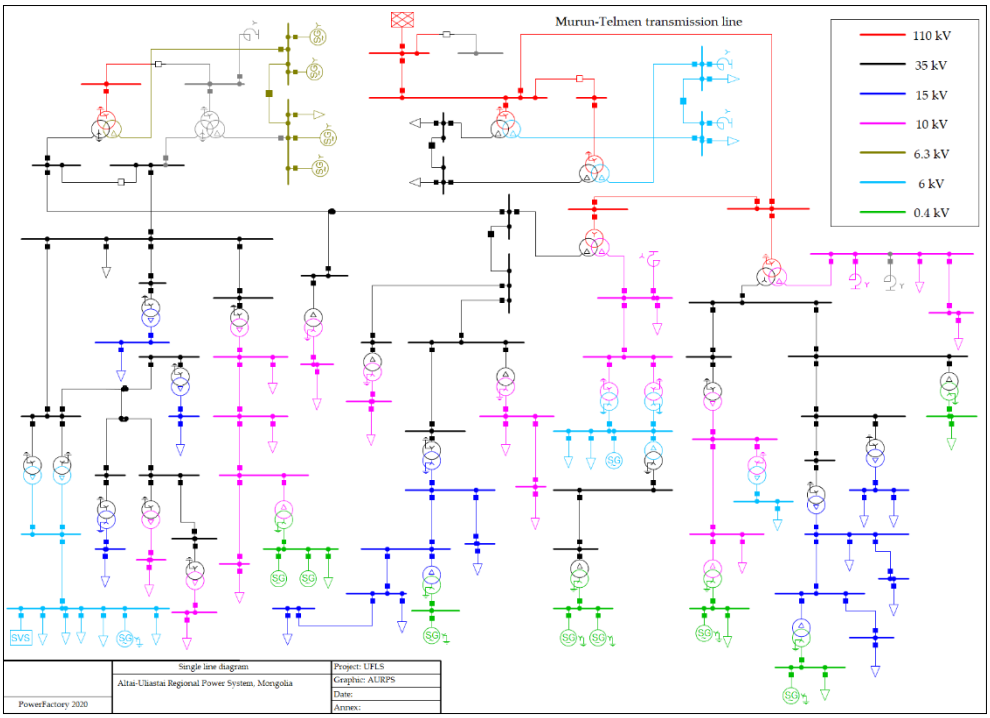

Figure 5. Schematic single-line diagram of Altai-Uliastai regional power system (AURPS).

The AURPS is radially interconnected to CRPS, and its power demand–supply highly depends on the power import from CRPS. Because the interconnector is exceptionally long, it is susceptible to frequent trips due to weather conditions. During interconnection outages, AURPS must be islanded and secure operation tried to be kept by activating the UFLS scheme. At this point, the islanded AURPS has a significant lack of power generation, and depending on the operational season (summer or winter), the inertia/demand levels significantly changes, directly impacting the UFLS performance. Currently, the traditional UFLS scheme of AURPS considers the same settings of UFRs for both operational seasons (summer and winter). However, the system operating conditions change significantly during winter compared to the summer season, as depicted in Table 1. During the winter season, local power production decreases 34.78%, and the power consumption increases 94.84% compared to the summer season. The decrease in power production and the increase in power demand in the winter season creates a significant reduction of system inertia. These operational conditions make the AURPS extremely vulnerable to any system event, and the UFLS scheme must be carefully adjusted to ensure secure operation of the AURPS. Consequently, in this paper, the settings of UFRs were computed for two operational scenarios: (i) high inertia—summer season, characterised by a high inertia level and low demand, and (ii) low inertia—winter season, characterised by a low inertia level and high demand requiring special attention in calculating the setting of UFRs.

The most significant frequency disturbance in the AURPS is the sudden disconnection of the Murun-Telmen 110 kV transmission line, causing a critical operational condition due to significant infeed loss. Therefore, this frequency event was used as the worst possible disturbance in AURPS. The sudden disconnection of the Murun-Telmen 110 kV transmission line was applied at t = 1.00 s.

The UFRs installed in the loads were based on a multi-step UFR, function ANSI 81, and the UFRs installed in the lines used the model SEL-751A provided in the DIgSILENT® PowerFactory™ Global Library. The UFRs of the loads only had one stage as in the real network; therefore, Ns = 1.

The boundaries of the frequency control variables were set following the technical and operational requirements of AURPS. f_{min} must not reach values below 47 Hz to avoid intervention of the UFP of the generators that are pre-set at 46.0 Hz; therefore, f_{limit} = 47 Hz. The continuous operating range of the generation units must be kept between 49.8 and 50.2 Hz; therefore $f_{ss,min}$ = 49.8 Hz and $f_{ss,max}$ = 50.2 Hz. The frequency threshold (f_t) should be between 47.6 and 49.4 Hz; therefore, F_{min} = 47.6

and F_{max} = 49.4 Hz. t_d should be at least six cycles (0.1 s) and should not exceed 18 cycles (0.3 s); therefore, T_{min} = 0.1 s and T_{max} = 0.3 s [29].

The set of parameters of IHS algorithm were set as those reported in the literature [37] as: *HMS* = 1.0, *HMCR* = 0.90, PAR_{min} = 0.35, PAR_{max} = 0.99, bw_{min} = 1×10^{-5}, bw_{max} = 1.0 and *NI* = 500.

7. Results

This section is dedicated to presenting the outcomes of assessing the optimal UFLS for high inertia—summer season and low inertia—winter season scenarios and discussing the results. Furthermore, sensitivity analysis is carried out to evaluate the optimal settings.

7.1. Optimal Settings of UFLS Scheme

7.1.1. High Inertia—Summer Season

The optimal setting of the UFRs for high inertia—summer season scenario obtained by computing the IHS algorithm are depicted in Table 3. Moreover, the objective function defined in (7), evaluated through 500 improvisations, is shown in the convergence curve in Figure 6. The optimal settings of UFRs produced a minimum load shedding of $P_{LS}(x_{FC})$ = 3.144 MW, which was reached in improvisation 303.

Table 3. Optimal UFLS settings of high inertia—summer season scenario of AURPS.

UFR Location	Element	ΔP (%)	f_T (Hz)	t_d (s)
Baynshand	Load	17.845	48.124	0.248
Baynhairhan	Load	43.595	48.644	0.244
Jargalant	Load	12.477	48.401	0.219
Uildwer	Load	29.740	48.784	0.210
Harzat	Load	9.733	47.986	0.188
Uliastai	Line	Open	49.317	0.220
Guulin	Line	Open	48.720	0.105
Biger garaa	Line	Open	48.661	0.126

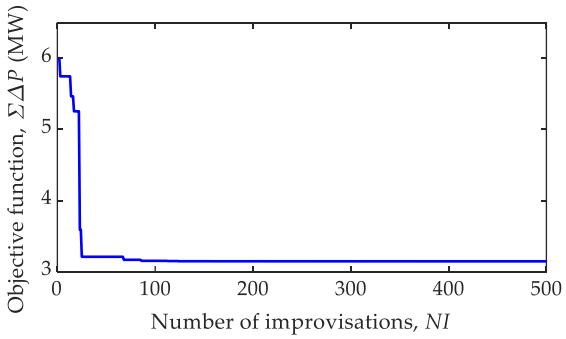

Figure 6. Convergence curve of optimal settings of UFRs for high inertia—summer season.

The dynamic response of the system frequency using the optimal settings of the UFLS scheme was computed and compared with the traditional UFLS scheme in AURPS. Figure 7 shows the frequency response comparison between the optimal UFLS and the traditional UFLS after the disconnection of the Murun-Telmen 110 kV transmission line. Moreover, Figure 8 depicts the active power of the loads and lines and also shows the trigger sequence of the UFRs during the outage.

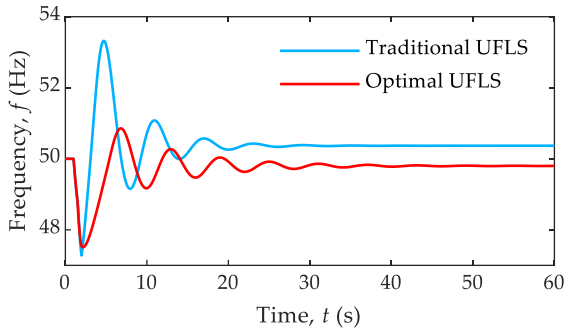

Figure 7. Frequency response in AURPS after disconnection of the Murun-Telmen 110 kV transmission line for high inertia—summer season scenario.

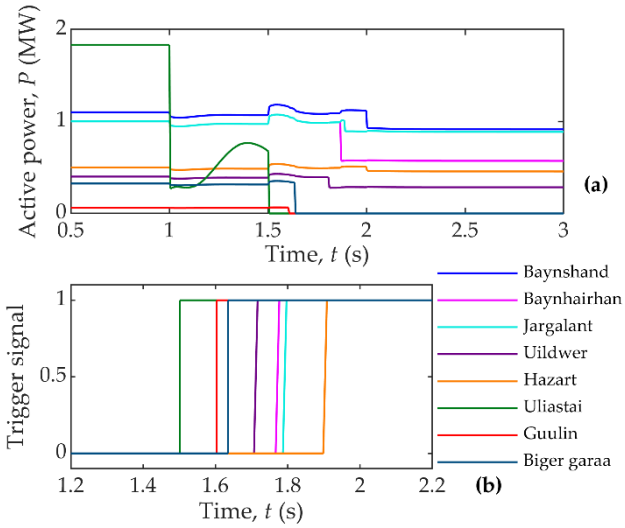

Figure 8. UFRs action in high inertia—summer season scenario: (**a**) active power; (**b**) trigger signal of the UFRs.

From Figure 7, it can be observed that the traditional UFLS scheme produced an over-frequency condition that caused the frequency to reach values above 53 Hz, which could result in activation of the over-frequency protection of the synchronous generators. The frequency quality metrics were computed to verify the positive improvements of the optimal UFLS scheme in the frequency response compared with the traditional UFLS, and the results are presented in Table 4. The optimal UFLS scheme prevented an unnecessary load shedding of 1.056 MW. It improved f_{min} by reducing the frequency depth by 0.232 Hz and avoided an over-frequency of continuing operation by settling the frequency at 49.8 Hz. The optimal setting of UFRs fulfilled the technical and operational constraints defined in (12).

Table 4. Frequency quality metrics of high inertia—summer season scenario.

UFLS Type	P_{LS} (MW)	f_{min} (Hz)	f_{ss} (Hz)	t_{min} (s)
Traditional	4.200	47.279	50.368	1.990
Optimal	3.144	47.511	49.800	2.160

7.1.2. Low Inertia—Winter Season

The disconnection of the Murun-Telmen 110 kV transmission line becomes extremely dangerous for the AURPS in low inertia—winter season scenario because demand is the maximum and small hydropower plants are out of service. Therefore, it is crucial to optimally compute the proper UFR settings.

The convergence curve of the objective function defined in (7) is presented in Figure 9. The IHS algorithm reached the minimum value at improvisation 348, indicating that optimal settings of UFRs depicted in Table 5 produced a minimum load shedding of $P_{LS}(x_{FC})$ = 4.803 MW.

Table 5. Optimal UFLS settings of low inertia—winter season scenario of AURPS.

UFR Location	Element	ΔP (%)	f_T (Hz)	t_d (s)
Baynshand	Load	84.818	49.003	0.264
Baynhairhan	Load	5.049	47.661	0.275
Jargalant	Load	72.712	48.816	0.108
Uildwer	Load	5.001	48.382	0.161
Harzat	Load	74.248	49.108	0.150
Uliastai	Line	Open	49.120	0.187

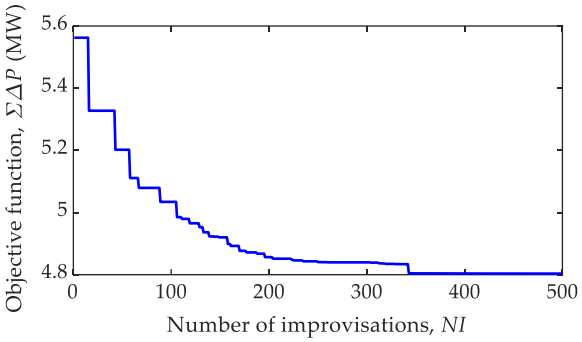

Figure 9. Convergence curve of optimal settings of UFRs for low inertia—winter season.

The optimal settings of the UFRs were evaluated by performing dynamic simulation of the AURPS model, applying a frequency event by disconnecting the Murun-Telmen 110 kV transmission line. Figure 10 shows the frequency response comparison between the traditional UFLS and the optimal UFLS. Using the traditional UFLS caused the minimum frequency to reach values below the frequency limit (f_{limit} = 47 Hz). This condition was caused by the inertia reduction, the increase in the power demand and the UFR parameters having the wrong setting. In contrast, the frequency response was improved by using the optimal settings, thereby avoiding activating UFP of the generators and a possible system collapse.

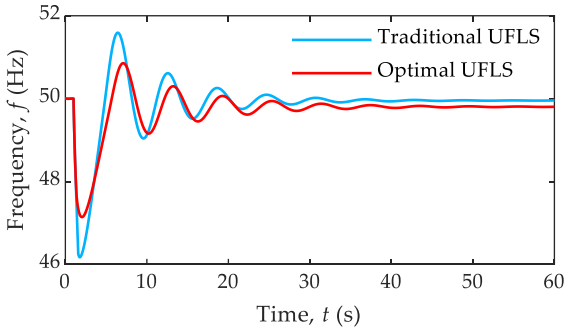

Figure 10. Frequency response in AURPS after disconnection of the Murun-Telmen 110 kV transmission line for low inertia—winter season scenario.

The active power disconnected and the trigger sequence of the UFRs during the outage are depicted in Figure 11. Before the UFR action, the negative value of active power in Uliastai indicates that the power flow direction has changed during the outage.

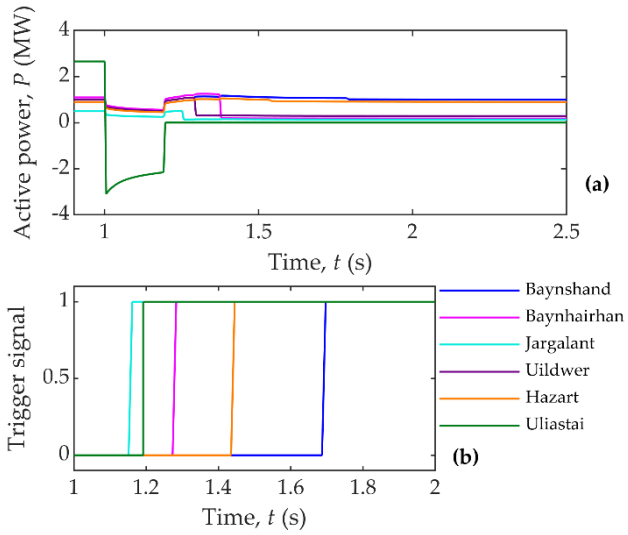

Figure 11. UFR action in low inertia—winter season scenario: (**a**) active power; (**b**) trigger signal of the UFRs.

Table 6 presents the frequency quality metrics of the optimal UFLS and traditional UFLS scheme. The optimal setting of UFRs significantly improved the frequency response by taking f_{min} out of the operating zone of UFP of generators, thus reducing the frequency depth by 0.978 Hz. Moreover, it prevented the unnecessary disconnection of 0.29 MW, and the frequency constraints defined in (12) were fulfilled.

Table 6. Frequency quality metrics of low inertia—winter season scenario.

UFLS Type	P_{LS} (MW)	f_{min} (Hz)	f_{ss} (Hz)	t_{min} (s)
Traditional	5.093	46.164	49.955	1.775
Optimal	4.803	47.142	49.804	2.038

7.2. Sensitivity Analysis

The optimal UFLS scheme formulation was focused on obtaining a set of optimal parameters (N_s, ΔP, f_T, t_d) for the UFRs that produce the minimum load disconnection during a frequency event and at the same time satisfy some frequency requirements. A sensitivity analysis was carried out to ensure that the resulting settings were optimal. This was done by decreasing the optimal block size of load shedding (ΔP) in all UFRs to demonstrate that another set of parameters (N_s, ΔP, f_T, t_d) did not exist for the UFRs that would cause minimum total load disconnection (calculated using (7)) and would satisfy the operational frequency requirements defined in (12).

The sensitivity analysis consisted of decreasing ΔP from 1% to 5% of its optimal values and observing the frequency quality metrics to ensure the set of parameters would meet the mentioned frequency constraints. The results of the sensitivity analysis are presented in Figure 12.

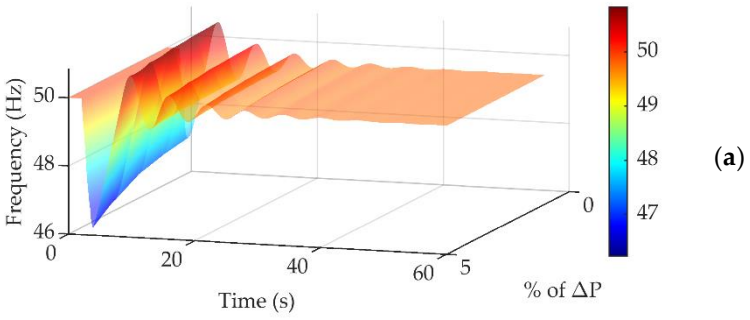

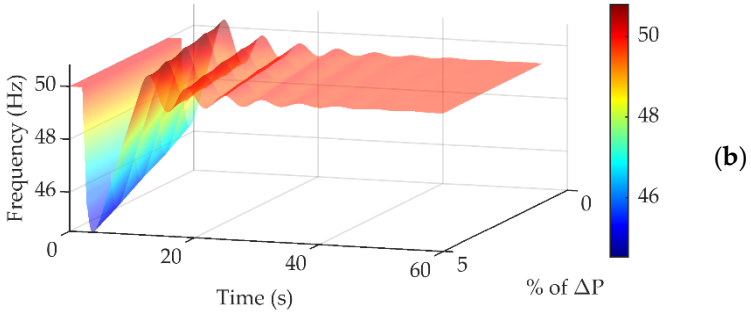

Figure 12. Frequency response by decreasing ΔP from 1% to 5%: (**a**) high inertia—summer season; (**b**) low inertia—winter season.

The sensitivity analysis for high inertia—summer season scenario, presented in Figure 12a, showed the steady-state frequency settled between 49.795 and 49.774 Hz for 1% and 5% of ΔP reduction, respectively, violating the constraints defined in (10), which determines that $f_{ss,min}$ must be greater or equal to 49.8 Hz. Moreover, the minimum frequency was between 47.384 and 46.222 Hz for 1 and 5% of ΔP reduction, respectively. Even though, for 1% of ΔP reduction f_{min} satisfied (10) and (11), the constraint of steady-state was not fulfilled. Meanwhile, for low inertia—winter season scenario, neither of the constraints defined in (12) were satisfied due to the minimum frequency falling below the frequency limit (f_{limit} = 47 Hz) and the steady-state frequency being lower than $f_{ss,min}$ for all percentages of ΔP reduction (see Figure 12b). Therefore, it has been proved that the UFLS parameters of high inertia—summer season and low inertia—winter season scenarios are optimal.

8. Conclusions

The optimal UFLS scheme developed in this paper allows computation of the optimal settings of UFRs and minimisation of the total amount of load shedding. Moreover, the set of frequency constraints that are defined to ensure the operational frequency requirements are satisfied, and the sensitivity analysis demonstrates that the calculated parameters of UFRs are globally optimal. This methodology can be used to calculate optimal settings of the UFLS scheme of any power system and allows the user to choose which variables they want to include in the optimisation process.

The computation of the UFR parameters of the UFLS scheme is carried out by applying a new approach that calculates the parameters of each UFR instead of assuming that UFRs have the same parameters. In this new methodology, the IHS metaheuristic algorithm is used; the set of frequency constraints defined in the optimal UFLS scheme allowing the minimum frequency as well as the steady-state frequency to be limited into desired values, even in significantly deteriorated operational scenarios, such as the ones with low inertia and high demand. This represents the main advantage as an unnecessary load shedding is prevented, and it is ensured that the frequency will be within the operational requirements of the power system.

The proposed optimal UFLS scheme was tested on the model of one regional power system belonging to the Mongolian power system, obtaining satisfactory results. The optimal UFLS scheme is suitable for replacement of the traditional UFLS scheme of AURPS as it was calculated using real data to model AURPS in DIgSILENT® PowerFactory™ and to perform the optimisation. Moreover, the optimal UFLS scheme overcomes the current UFLS scheme of AURPS, providing optimal settings for two operational scenarios: high and low inertia.

Author Contributions: Conceptualisation, F.G.-L., M.A.A., J.R.T., C.A. and M.N.A.; methodology, F.G.-L., M.N.A. and C.A.; software, M.N.A.; validation, F.G.-L., M.A.A., J.R.T., J.M.R.S. and E.V.; formal analysis, M.N.A., F.G.-L., M.A.A. and J.R.T.; investigation, M.N.A. and C.A.; resources, F.G.-L.; data curation, M.N.A. and C.A.; writing—original draft preparation, M.N.A.; writing—review and editing, F.G.-L., C.A., M.A.A., J.R.T., J.M.R.S. and E.V.; visualisation, M.N.A. and C.A.; supervision, F.G.-L., M.A.A., J.R.T., J.M.R.S. and E.V. All authors have read and agreed to the published version of the manuscript.

Funding: This research received no external funding.

Acknowledgments: Martha N. Acosta acknowledges the financial support given by CONACYT (Mexico) and would like to thank the support of the University of South-Eastern Norway and Universidad Autónoma de Nuevo León. Choidorj Adiyabazar wants to acknowledge the financial support given by National Dispatching Centre of Mongolia Co., Ltd. and the University of South-Eastern Norway. F. Gonzalez-Longatt would like to express his gratitude to DIgSILENT GmbH for supporting his research.

Conflicts of Interest: The authors declare no conflict of interest.

References

1. Gonzalez-Longatt, F.M. Impact of emulated inertia from wind power on under-frequency protection schemes of future power systems. *J. Mod. Power Syst. Clean Energy* **2016**, *4*, doi:10.1007/s40565-015-0143-x.
2. Omar, Y.R.; Abidin, I.Z.; Yusof, S.; Hashim, H.; Abdul Rashid, H.A. Under Frequency Load Shedding (UFLS): Principles and implementation. In Proceedings of the PECon2010—2010 IEEE International Conference on Power and Energy; Kuala Lumpur, Malaysia, 29 November–1 December 2010; pp. 414–419.
3. Sigrist, L.; Rouco, L.; Echavarren, F.M. A review of the state of the art of UFLS schemes for isolated power systems. *Int. J. Electr. Power Energy Syst.* **2018**, *99*, 525–539, doi:10.1016/j.ijepes.2018.01.052.
4. Acosta, M.N.; Andrade, M.A.; Vazquez, E.; Adiyabazar, C.; Gonzalez-Longatt, F.; Rueda, J..; Palensky, P. Improvement of the Frequency Response Indicators by Optimal UFLS Scheme Settings. In Proceedings of the 2020 IEEE 29th International Symposium on Industrial Electronics (ISIE); IEEE: Hague, Netherlands, 17–19 June 2020; pp. 1250–1255.
5. Hafez, A.A.; Hatata, A.Y.; Abdelaziz, A.Y. Multi-Objective Particle Swarm for Optimal Load Shedding Remedy Strategies of Power System. *Electr. Power Components Syst.* **2019**, *47*, 1651–1666, doi:10.1080/15325008.2019.1689454.
6. IEEE *IEEE Std C37.117 - IEEE Guide for the Application of Protective Relays Used for Abnormal Frequency Load Shedding and Restoration*; IEEE: Piscataway, NJ, USA, 2007; ISBN 073815539X.
7. Ketabi, A.; Hajiakbari Fini, M. Adaptive underfrequency load shedding using particle swarm optimization algorithm. *J. Appl. Res. Technol.* **2017**, *15*, 54–60, doi:10.1016/j.jart.2016.12.003.
8. Laghari, J.A.; Mokhlis, H.; Karimi, M.; Abu Bakar, A.H.; Mohamad, H. A New Under-Frequency Load Shedding Technique Based on Combination of Fixed and Random Priority of Loads for Smart Grid Applications. *IEEE Trans. Power Syst.* **2015**, *30*, 2507–2515, doi:10.1109/TPWRS.2014.2360520.
9. Fernandes, R.V.; De Almeida, S.A.B.; Maciel Barbosa, F.P.; Pestana, R. Load shedding—Coordination between the Portuguese transmission grid and the distribution grid with minimization of loss of distributed generation. In Proceedings of the 2009 IEEE Bucharest PowerTech: Innovative Ideas Toward the Electrical Grid of the Future; Bucharest, Romania, 28 June–2 July 2009.
10. Mollah, K.U.Z.; Bahadornejad, M.; Nair, N.K. Automatic under-frequency load shedding in New Zealand power system—A systematic review; IEEE Conference Publication: Piscataway, NJ, USA, 2011.
11. Rudez, U.; Mihalic, R. Dynamic analysis of transition into island conditions of Slovenian power system applying underfrequency load shedding scheme. In Proceedings of the 2009 IEEE Bucharest PowerTech: Innovative Ideas Toward the Electrical Grid of the Future; Bucharest, Romania, 28 June–2 July 2009.
12. Hong, Y.Y.; Chen, P.H. Genetic-based underfrequency load shedding in a stand-alone power system considering fuzzy loads. *IEEE Trans. Power Deliv.* **2012**, *27*, 87–95, doi:10.1109/TPWRD.2011.2170860.
13. Yan, J.; Li, C.; Liu, Y. Adaptive load shedding method based on power imbalance estimated by ANN. In Proceedings of the TENCON 2017—2017 IEEE Region 10 Conference, Penang, Malaysia, 5–8 November 2017; Volume 2017-Decem, pp. 2996–2999.
14. Huang, B.; Du, Z.; Liu, Y.; Zhao, F. Study on online under-frequency load shedding strategy with virtual inertia control of wind turbines. *J. Eng.* **2017**, *2017*, 1819–1823, doi:10.1049/joe.2017.0645.
15. Drabandsari, A.; Amraee, T. Optimal Setting of Under Frequency Load Shedding Relays in Low Inertia Networks. In Proceedings of the 2018 Smart Grid Conference (SGC), Kurdistan, Iran, 28–29 November 2018; pp. 1–6.
16. Lytvynchuk, V.A.; Kaplin, M.I.; Bolotnyi, N.P. The Method of Design an Optimal Under-Frequency Load Shedding Scheme. In Proceedings of the 2019 IEEE 6th International Conference on Energy Smart Systems, ESS 2019—Proceedings, Kyiv, Ukraine, 17–19 April 2019; Vol. 1, pp. 14–17; doi:10.1109/ESS.2019.8764241.

17. Abedini, M.; Sanaye-Pasand, M.; Azizi, S. Adaptive load shedding scheme to preserve the power system stability following large disturbances. *IET Gener. Transm. Distrib.* **2014**, *8*, 2124–2133, doi:10.1049/iet-gtd.2013.0937.
18. Zhang, X.; Ma, J.; Yao, S.; Chen, R. Optimization method of under frequency load shedding schemes for systems with high permeability new energy. In Proceedings of the 2019 4th International Conference on Intelligent Green Building and Smart Grid, IGBSG 2019, Yichang, China, 6–9 September 2019; pp. 577–580; doi:10.1109/IGBSG.2019.8886196.
19. Mohamad, H.; Isa, A.I.M.; Yasin, Z.M.; Salim, N.A.; Rahim, N.N.A.M. Optimal load shedding technique for an islanding distribution system by using Particle Swarm Optimization. In Proceedings of the 3rd International Conference on Power Generation Systems and Renewable Energy Technologies, PGSRET 2017, Johor Bahru, Malaysia, 4–6 April 2017; pp. 154–158 ; doi:10.1109/PGSRET.2017.8251819.
20. Xu, X.; Zhang, H.; Chai, Y.; Shi, F.; Li, Z.; Li, W. Trajectory sensitivity-based emergency load shedding optimal algorithm. In Proceedings of the Proceedings of the 5th IEEE International Conference on Electric Utility Deregulation, Restructuring and Power Technologies, DRPT 2015, Changsha, China, 26–29 November 2015; pp. 1368–1372; doi:10.1109/DRPT.2015.7432444.
21. Shun, L.; Qingfen, L.; Jiali, W. Dynamic optimization of adaptive under-frequency load shedding based on WAMS. In Proceedings of the Proceedings of 2016 IEEE Information Technology, Networking, Electronic and Automation Control Conference, ITNEC 2016, Chongqing, China, 20–22 May 2016; pp. 920–926.
22. Wang, J.; Zhang, H.; Zhou, Y. Intelligent under Frequency and under Voltage Load Shedding Method Based on the Active Participation of Smart Appliances. *IEEE Trans. Smart Grid* **2017**, *8*, 353–361, doi:10.1109/TSG.2016.2582902.
23. Jianjun, Z.; Dongyu, S.; Dong, Z.; Yang, G. Load Shedding Control Strategy for Power System Based on the System Frequency and Voltage Stability. In Proceedings of the 2018 China International Conference on Electricity Distribution (CICED), Tianjin, China, 17–19 September 2018; pp. 1352–1355.
24. Alhelou, H.H.; Golshan, M.E.H.; Zamani, R.; Moghaddam, M.P.; Njenda, T.C.; Siano, P.; Marzband, M. An improved UFLS scheme based on estimated minimum frequency and power deficit. In Proceedings of the 2019 IEEE Milan PowerTech, PowerTech 2019, Milano, Italy, 23–27 June 2019.
25. Haes Alhelou, H.; Hamedani Golshan, M.; Njenda, T.; Siano, P. WAMS-Based Online Disturbance Estimation in Interconnected Power Systems Using Disturbance Observer. *Appl. Sci.* **2019**, *9*, 990, doi:10.3390/app9050990.
26. Alhelou, H.; Hamedani-Golshan, M.; Njenda, T.; Siano, P. Wide-Area Measurement System-Based Optimal Multi-Stage Under-Frequency Load-Shedding in Interconnected Smart Power Systems Using Evolutionary Computing Techniques. *Appl. Sci.* **2019**, *9*, 508, doi:10.3390/app9030508.
27. Haes Alhelou, H.; Hamedani Golshan, M.E.; Njenda, T.C.; Hatziargyriou, N.D. An Overview of UFLS in Conventional, Modern, and Future Smart Power Systems: Challenges and Opportunities. *Electr. Power Syst. Res.* **2020**, *179*, 106054, doi:10.1016/j.epsr.2019.106054.
28. Adiyabazar, C.; Acosta, M.N.; Gonzalez-Longatt, F.; Rueda, J.L.; Palensky, P. Under-Frequency Load Shedding in Mongolia: Simulation Assessment Considering Inertia Scenarios. In Proceedings of the 2020 IEEE 29th International Symposium on Industrial Electronics (ISIE); IEEE: Delft, Netherlands, 17–19 June 2020; pp. 1256–1261.
29. Profileprojections, S.; Generation, C.; Energy, R.; Expansion, C. *Strategy for NAPSI Technical Assistance for Mongolia - RENEWABLE ENERGY CAPACITY EXPANSION PLAN*; ADB: Mandaluyong, Philippines, 2018;.
30. Gonzalez-Longatt, F.; Sanchez, F.; Leelaruji, R. Unveiling the Character of the Frequency in Power Systems. In Proceedings of the 2019 IEEE PES GTD Grand International Conference and Exposition Asia (GTD Asia), Bangkok, Thailand, 20–23 March 2019; pp. 57–62.
31. Acosta, M.N.; Pettersen, D.; Gonzalez-Longatt, F.; Peredo Argos, J.; Andrade, M.A. Optimal Frequency Support of Variable-Speed Hydropower Plants at Telemark and Vestfold, Norway: Future Scenarios of Nordic Power System. *Energies* **2020**, *13*, 3377, doi:10.3390/en13133377.
32. IEEE *IEEE Std C37.111 IEEE Guide for AC Generator Protection*; IEEE: Piscataway, NJ, USA, 2013; Volume 2006; ISBN 9782832207666.
33. IEEE IEEE Std C37.106. Guide for Abnormal Frequency Protection for Power Generating Plants. In *IEEE*; IEEE: Piscataway, NJ, USA, 2004; pp. 1–34; doi:10.1109/IEEESTD.2004.94434.

34. Zong Woo Geem; Joong Hoon Kim; Loganathan, G.V. A New Heuristic Optimization Algorithm: Harmony Search. *Simulation* **2001**, *76*, 60–68, doi:10.1177/003754970107600201.
35. Lee, K.S.; Geem, Z.W. A new meta-heuristic algorithm for continuous engineering optimization: Harmony search theory and practice. *Comput. Methods Appl. Mech. Eng.* **2005**, *194*, 3902–3933, doi:10.1016/j.cma.2004.09.007.
36. Biscani, F.; Izzo, D. esa/pagmo2: Pagmo 2.14.0. Available online: https://zenodo.org/record/3697219 (accessed on Mar 13, 2020).
37. Improved Harmony Search (IHS)—Pagmo 2.15.0 documentation Available online: https://esa.github.io/pagmo2/docs/cpp/algorithms/ihs.html#_CPPv4N5pagmo3ihsE (accessed on 13 March 2020).